

GNNAnatomy: Systematic Generation and Evaluation of Multi-Level Explanations for Graph Neural Networks

Hsiao-Ying Lu, Yiran Li, Ujwal Pratap Krishna Kaluvakolanu Thyagarajan, Kwan-Liu Ma

Abstract—

Graph Neural Networks (GNNs) excel in machine learning tasks involving graphs, such as node classification, graph classification, and link prediction. However, explaining their decision-making process is challenging due to the complex transformations GNNs perform by aggregating relational information from graph topology. Existing methods for explaining GNNs face key limitations: (1) lack of flexibility in generating explanations at varying levels, (2) difficulty in identifying unique substructures relevant to class differentiation, and (3) little support to ensure the trustworthiness of explanations. To address these challenges, we introduce GNNAnatomy, a visual analytics system designed to generate and evaluate multi-level GNN explanations for graph classification tasks. GNNAnatomy uses graphlets—primitive graph substructures—to identify the most critical substructures in a graph class by analyzing the correlation between GNN predictions and graphlet frequencies. These correlations are presented interactively for user-selected group of graphs through our visual analytics system. To further validate top-ranked graphlets, we measure the change in classification confidence after removing each graphlet from the original graph. We demonstrate the effectiveness of GNNAnatomy through case studies on synthetic and real-world graph datasets from sociology and biology domains. Additionally, we compare GNNAnatomy with state-of-the-art explainable GNN methods to showcase its utility and versatility.

Index Terms—Graphlets, Motif, Graph Neural Network, Explainable AI, Visual Analytics, Visualization

1 INTRODUCTION

Graph Neural Networks (GNNs) have become increasingly prominent for their state-of-the-art performance in graph data tasks, impacting various domains such as social network analysis [1, 8, 28, 37] and biological science research [15, 23, 29]. GNNs convert complex graph structures into vector representations by aggregating relational information from neighboring nodes [18, 48], capturing intricate topological features that enable accurate predictions or classifications. While achieving high accuracy is crucial, interpretability is equally essential for real-world applications of GNNs. For example, in teamwork graphs where nodes represent participants and edges signify collaborations, and labels of graphs indicate historical success or failure, GNNs can effectively classify outcomes based on structural characteristics. However, simply knowing the predicted outcome is not enough. To derive actionable insights, such as planning interventions to prevent undesirable outcomes, it is essential to uncover and understand the specific topological traits GNNs use for class differentiation. Integrating interpretability into GNNs not only enhances trust and transparency in their predictions but also equips decision-makers with the knowledge to optimize results in complex, real-world scenarios.

Existing explainable GNN methods can be summarized as follows. To understand a trained GNN’s behavior, first, the *level* of explanation is determined, which pertains to whether to identify the important graph components in a single graph instance [11, 14, 35, 39, 42, 47, 52, 53] or within a class of graphs [4, 44]. Then, the *format* of a explanation is decided based on the choice of level, which can be a subgraph explanation for a graph instance [11, 14, 27, 30, 35, 39, 42, 47, 52, 53] or a set of substructure explanations containing the common patterns exhibited by graphs within the same class [46, 49]. Finally, these generated explanations require *evaluation*, where metrics [2, 13, 25, 31, 31, 34, 47] are applied and the scores are compared among different explainable GNN methods.

Each step of the aforementioned process presents key limitations. To begin with, most explainable GNN methods produce instance-level explanations, typically as subgraphs for individual graph instances. These explanations are tailored to a specific GNN prediction and may not generalize across other graphs, limiting their ability to offer a

comprehensive understanding of GNN behavior. Class-level explanations, which identify common substructures within specific classes, also fall short—they may not highlight the most distinguishing patterns that help GNNs differentiate between classes. Additionally, many explainable GNN methods rely on another ML model to generate explanations [43, 46, 47, 49]. These explanations are often compared based on metric scores, but even when achieving higher scores, they may still be unconvincing to decision-makers seeking to understand GNN behavior. Using another ML model to explain GNNs only shifts the trust issue from the GNN to its explainer, rather than resolving it.

To address the need for GNN interpretability and tackle existing challenges, we introduce GNNAnatomy, a visual analytics system for generating and evaluating GNN explanations. GNNAnatomy employs *graphlets* as explanatory elements, representing each graph as a vector of graphlet occurrence frequencies, which characterize the diverse fundamental substructures within the graph. GNNAnatomy illustrates the relationship between GNN classifications and graphlet frequencies, guiding users to identify groups of graphs that rely on different substructures for class differentiation within each group. This approach overcomes the constrain of instance- and class-level explanations, enabling GNNs to be explained at flexible, user-defined levels. GNNAnatomy ranks the relevance of each graphlet by correlating its frequency with GNN classifications, revealing the substructure that contributes to class differentiation. To further evaluate the validity of the top-ranked graphlet, its relevance is confirmed by measuring the change in classification confidence after removing the graphlet substructure from the original graph. In this way, users can explore both the correlation coefficient and classification confidence changes for each graphlet, ensuring the trustworthiness of the top-ranked substructure explanation.

We demonstrate the effectiveness of GNNAnatomy through case studies on real-world and synthetic graph datasets across different domains, comparing the explanations it generates with those from state-of-the-art explainable GNN methods. These case studies showcase GNNAnatomy’s ability to capture compact and intrinsic topological differences between classes. Overall, our contributions include:

- Enabling the generation of explanations for GNNs at flexible levels,
- Identifying distinguishing substructures that contribute to class differentiation made by GNNs,
- Enhancing the trustworthiness of explanations by allowing free exploration of the relevance of diverse substructures, and

• All authors are with University of California, Davis. E-mail: {hyllu, ranli, ujwkal, klma}@ucdavis.edu.

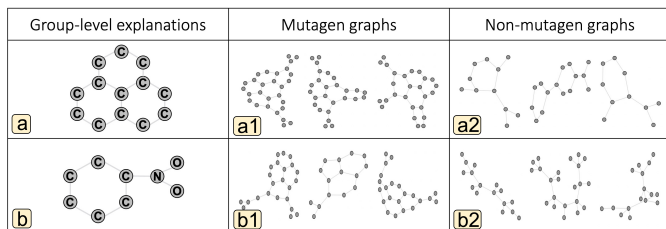


Fig. 1: An example showing mutagens may exhibit different mutagenic compounds that distinguish them from non-mutagens.

- Delivering GNNAnatomy, a model- and domain-agnostic visual analytics system that supports the interactive generation and evaluation of GNN explanations at desired levels.

2 RELATED WORKS

With the growing success of employing graph neural networks (GNNs) in tasks involving graph-structured data, the importance of interpreting GNNs has also increased. In this section, we discuss previous approaches and highlight the remaining challenges across three key stages in the pipeline of explainable GNN methods: explanation level, format, and evaluation. Finally, we review visual analytics works that contribute to explaining GNNs behavior.

2.1 Level of Explanation

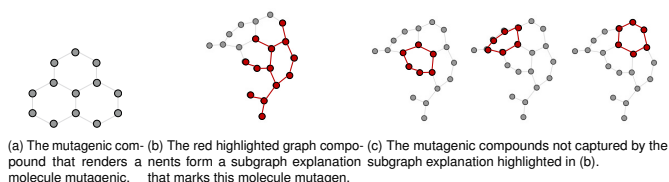
As outlined in a recent survey [51], explainable GNN methods generally produce either instance-level or model-level (class-level) explanations. Instance-level methods focus on identifying a subgraph most relevant to the GNN’s prediction for each graph instance, while class-level approaches aim to provide common substructure(s) as explanations for each class. Most existing research focuses on explaining GNN predictions at the instance level [11, 14, 35, 39, 42, 47, 52, 53]. However, instance-level explanations may not be applicable to other graph instances, limiting their ability to provide a general understanding of GNN behavior.

Conversely, class-level methods aim to provide common patterns within each class as explanations. Xuanyuan et al. [44] treat neurons in GNNs as concept detectors that generalize across multiple graph instances. XGNN [50] learns a graph generator that produces graphs containing the most critical substructures for each class, maximizing the classification confidence of a trained GNN. D4Explainer [4] uses reverse sampling and a denoising model to optimize the generation of class-wise explanations. However, these class-level topological patterns may not capture the most distinguishing substructures that enable GNNs to differentiate between classes, highlighting the need for finer-grained details to improve the interpretability of GNN behavior.

Additionally, different sets of graphs may require distinct topological traits for effective class differentiation. For instance, in classifying a molecule’s mutagenicity, both fused carbon rings and NO_2 attached to a carbon ring are known mutagenic compounds [6], as illustrated in Fig. 1(a, b). In the group of graphs shown in Fig. 1(a1, a2), the fused carbon ring structure is exclusively present in Mutagen graphs, making it the key distinguishing feature within this group. Conversely, in the group shown in Fig. 1(b1, b2), the most distinguishing feature is the presence of an NO_2 group attached to a carbon ring, which is absent in Non-mutagen graphs. Thus, to effectively explain GNN behavior, it is crucial to offer explanations at varying levels of detail by identifying groups of graphs with distinct structural traits and determining the most distinguishing substructure for class differentiation within each group.

2.2 Format of Explanation

Most existing explainable GNN methods generate instance-level explanations, typically in the form of a **subgraph** that has the most significant influence on GNN predictions. We review these methods based on their approaches. Perturbation-based methods [11, 27, 35, 42, 47, 52] use trained generators to produce masks (e.g., node or edge masks) that perturb the input graphs. These masks retain only the critical structural information necessary to preserve similar GNN predictions to



(a) The mutagenic compound that renders a molecule mutagenic. (b) The red highlighted graph component that marks this molecule mutagenic. (c) The mutagenic compounds not captured by the subgraph explanation highlighted in (b).

Fig. 2: An example of how a subgraph explanation can be misleading due to imprecise.

the original graphs. Surrogate-based methods [14, 30, 39, 53] rely on simpler, interpretable surrogate models to approximate GNN predictions using local neighboring data derived from input graphs, providing interpretable insights into GNN behavior.

However, using subgraphs as explanations can be misleading, as they hinder the understanding of key topological motifs. For instance, in the molecule mutagenicity classification task, fused ring structures, as shown in Fig. 2(a), are known to contribute to a molecule’s mutagenicity [6]. Ideally, an explanation subgraph should include this motif. However, as highlighted in red in Fig. 2(b), the explanation subgraph captures only one ring while including extra, irrelevant atoms. These additional atoms may mislead analysts into attributing undue significance to them, while the absence of the other rings fused together, as shown in Fig. 2(c), may create confusion regarding the true importance of this substructure. To prevent such issues, a more effective approach is to directly identify the relevant **substructure** (e.g., fused rings) as the explanation, rather than subgraphs.

To generate explanatory substructures (motifs), a set of substructures must first be defined. In biological graphs representing molecules, domain knowledge is often applied to create hand-crafted rules that define motifs as molecular fragments [7, 21]. Another approach, applicable to more general graphs, focuses on identifying motifs from ring-structured patterns [3, 16]. Additionally, Wang et al. [43] use contrastive learning [5] to extract class-specific common patterns. However, these motifs are typically domain- or dataset-specific, or they only capture limited types of topological structures. Moreover, such motif extraction methods are seldom utilized in explainable GNN research.

MotifExplainer [49] is one effort to identify the most explanatory, domain-specific motifs using an attention-based model. However, it still provides subgraph explanations by decomposing the original graphs into components, rather than directly identifying relevant substructures. In contrast, Yin et al. [46] propose a structural pattern learning module that extracts universal graph patterns, identifying the most explanatory substructure across a dataset. However, this method relies on pre-defined ground truth motifs, which are rarely available in real-world applications. Thus, a challenge remains: defining a diverse set of substructures that characterizes topologies across domains and identifying the most explanatory one among this set.

2.3 Evaluation of GNN Explanations

Evaluations are essential for verifying the validity of generated explanations. Existing GNN explainers employ machine learning (ML) models to generate explanations and utilize metric scores to quantify and compare the validity of these explanations against those from other explainers. These metrics include accuracy measures like F1 or ROC-AUC scores [34, 47], which rely on the availability of ground truth. Fidelity metrics [13, 31] assess the change in GNN predictions when the explanation is removed from the original graph. Sparsity metrics [31] focus on the compactness of the explanations, requiring them to have minimal impact on graph size and edge density when removed. Some metrics combine multiple concepts from the above metrics to provide a more robust evaluation [2, 25].

Even when an explanation achieves high metric scores, it can still be unconvincing because it is generated by another black-box ML model. Explainable GNN research is gaining attention not only for its ability to derive actionable insights but also due to the trust issues faced by users of the trained ML models. Relying on another ML model to explain the black-box GNN simply transfers these trust issues from the GNN to its explainer. A more effective approach would be to

provide ample evidence that guides users in reasoning about the GNN’s behavior and arriving at a trustworthy explanation. To achieve this, visual analytics (VA) has proven to be an effective technique, allowing users to interactively explore and interpret complex data. We discuss the contributions of VA in explaining GNNs in the next section.

2.4 Visual Analytics for Explaining GNNs

Recent surveys [20, 40] highlight a growing interest in visual analytics (VA) within explainable ML research, though only a small portion specifically targets GNN explainability. For instance, EmbeddingVis [22] facilitates correlation analysis within a VA system to explore node metrics preserved in GNN-learned embeddings. Emb-comp [12] provides an interface for comparing embeddings, helping users understand how different GNNs model graph data. Liu et al. [24] propose a K-hop graph layout that links node embeddings to their topological neighborhoods for diagnosing GNN models. Similarly, GNNLens [17] was developed to explain and diagnose GNN predictions by analyzing correlations between nodes and their neighbors.

However, these methods fall short of offering intuitive explanations that allow users to quickly grasp the topological or semantic features key to a GNN’s predictions. Instead, these VA tools provide ample evidence but rely on users to extract meaningful insights and construct their own explanations. This can lead to inconsistent interpretations, making it difficult to assess the validity of the explanations.

In contrast, Wang et al. [41] developed a drug repurposing visual analytics system that utilizes GraphMask [35] to extract critical meta-paths, making the results interpretable for domain experts. Similar to our approach, this work emphasizes the importance of generating GNN explanations at varying levels of detail. While it succeeds in providing clear explanations that are understandable within a specific domain, its visualization design choices are heavily customized to domain-specific needs, limiting the system’s generalizability to other graph datasets and different GNN architectures.

3 BACKGROUND

This work employs graphlets to explain the behavior of graph neural networks (GNNs) in graph-level classification tasks. In this section, we offer concise background information on the two techniques.

3.1 Graphlets and Graphlet Frequencies

Graphlets are small connected non-isomorphic graphs [9, 32]. Given a specific number of nodes in a graphlet, there is a fixed number of graphlet types. For example, we show all 6 graphlet types with 4 nodes in Fig. 3. Graphlets have been used in both analysis and visualization of graphs/networks [19, 38].

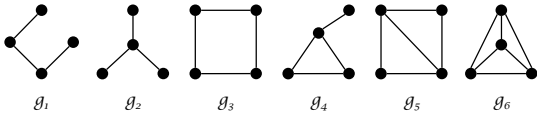


Fig. 3: Six graphlet types with four nodes.

The relative frequencies of different graphlet types can be used to characterize the topology of a graph. If we would use the 6 graphlet types g_1, g_2, \dots, g_6 in Fig. 3 to characterize a set of graphs, a 6D vector of graphlet frequencies \mathbf{f}_G is extracted to represent the graphlet distribution in each graph G :

$$\mathbf{f}_G = (f_{g_1}, f_{g_2}, \dots, f_{g_6}), \quad (1)$$

where

$$f_{g_k} = \frac{\#(g_k \subseteq G)}{\sum_{i=1}^6 \#(g_i \subseteq G)}. \quad (2)$$

3.2 Graph Neural Networks

Graph Neural Networks (GNNs) are machine learning models designed to operate on graph-structured data, enabling them to capture the relational characteristics inherent in graphs. They learn structure-aware node representations by iteratively gathering information from a node’s

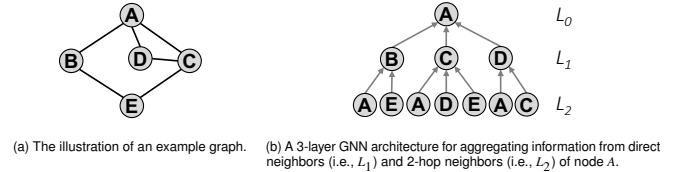


Fig. 4: The process of relational information aggregation in GNNs.

neighbors. In each iteration, a node aggregates information from its directly connected neighbors. This aggregated information is then integrated with the node’s current representation. Taking the graph illustrated in Fig. 4(a) as an example, a GNN may update node A’s representation through multiple layers of aggregation as shown in Fig. 4(b). After the input layer, L_2 obtains the current representations of the 2-hop neighbors (i.e., the nodes connected to A’s direct neighbors). These representations are aggregated and then combined with the current representations of A’s direct neighbors in L_1 . The combined representations of nodes B, C, and D are again aggregated and then merged with node A’s current representation in L_0 , concluding the update process for node A. Consequently, the number of layers in GNNs determines how far the node information propagates within the graph through edge connections.

This process is repeated for every node in the graph, resulting in learned node representations/embeddings that are more manageable for performing graph-related downstream tasks such as node classification, edge prediction, or graph classification. For graph classification tasks, the embeddings of all nodes are further aggregated into a single graph embedding, which serves as the input to the downstream classifier.

4 METHODOLOGY

As outlined in Sec. 2, existing explainable GNN methods face key limitations in three areas: (1) explanation level, (2) format, and (3) evaluability. In this section, we describe our solutions for addressing these challenges. These challenges of explaining GNNs is intricately tied to understanding graph structures rather than just node or edge features, as also noted by [27]. Additionally, uncovering relevant features for non-graph neural networks is a well-studied field [10, 26, 33]. Thus, our work focuses on identifying the graph substructures most relevant to GNN behavior.

4.1 Graphlet Frequency: Topological Summary

As outlined in Sec. 3.1, our method employs graphlets to characterize each graph’s topology into graphlet frequency vector. In the actual computation of graphlet frequencies, it is too time-consuming to count the exact occurrence of each graphlet because comparing all possible connected subgraphs is an NP-hard problem. Therefore, we adopt the connected subgraph sampling method in [36], and compute the frequency of each type of graphlet among a set of subgraphs (with 3, 4, and 5 nodes) sampled from G . For any graph G , we concatenate the 2D vector of the 3-node graphlet frequencies, the 6D vector of the 4-node graphlet frequencies, and the 21D vector of the 5-node graphlet frequencies into a single 29D graphlet representation.

Each dimension in the 29D graphlet frequency vector represents the relative occurrence of a specific graphlet type within a graph. The frequency of the same graphlet across different graphs depends on factors such as the graph’s size (i.e., the number of nodes), the number of sampled subgraphs, and the occurrence count of that graphlet. Given that there are 112 types of 6-node graphlets alone, distinguishing between them becomes challenging for users. Therefore, our approach focuses on 3-, 4-, and 5-node graphlets, providing a diverse yet comprehensible structural representation of graph topology. Additionally, GNN architectures rarely exceed 4 layers, making it unlikely for graphlet substructures with more than 5 nodes to be captured effectively by GNNs. If additional graphlets are required due to domain consideration, their frequencies can be easily concatenated into the original graphlet frequency vector for extended analysis.

The use of graphlets offers several advantages for explainable GNN analysis. First, unlike existing motif extraction methods [3, 5, 16, 43],

graphlets capture a diverse range of substructures and can be applied to any graph without relying on domain-specific knowledge for extraction rules. Second, graphlets provide a concise topological representation, the graphlet frequency vector, which simplifies the subsequent explanation process. In contrast to previous approaches with machine learning models transforming extracted motifs into uninterpretable vector representations [46, 49], the graphlet frequency vector is both semantically understandable and directly derived from the original graphs. Lastly, the compact size of graphlets makes them intuitive to interpret and easily distinguishable from one another.

4.2 Surrogate Model: Explanation Fidelity Evaluation

4.2.1 Surrogate Model Architecture and Training

A common way to evaluate an explanation is to measure the impact of removing involved nodes and edges on GNN’s prediction, such as the Fidelity metric [31]. To adapt this approach for our explanatory substructures, we leverage graphlet frequency vectors and design a surrogate model to approximate GNN behavior. Specifically, an encoder-decoder model is trained to reconstruct GNN-generated graph embeddings from graphlet frequency vectors. Since these vectors are directly extracted from the original graphs, they offer a comprehensive dataset representation. While connected graphlets may not capture disconnected topology, they effectively approximate the GNN’s aggregation mechanism, which also only gather information iteratively from neighbors (i.e., connected nodes).

For each graph, we use its 29D graphlet frequency vector as input to the *encoder*. This passes through two 20D hidden layers, producing a 10D bottleneck latent vector. The bottleneck restricts the model from memorizing the mapping between graphlet frequencies and graph embeddings by significantly reducing the raw input. The latent vector then goes through a linear layer and softmax function, generating 2D classification probabilities. The *encoder* is trained using L2 reconstruction loss to match the GNN’s classification outputs. The *decoder* takes the latent vector as input and reconstructs the graph embedding through two 20D hidden layers, incorporating bypassed outputs from the symmetrical residual connections to the *encoder*. This reconstructed embedding is passed to a fixed classification model, trained alongside the GNN, to convert the embedding into 2D classification probabilities. The *decoder* is trained with L2 reconstruction losses from both the graph embedding and the classification probabilities.

We train our encoder-decoder model by alternating between training the *encoder* and *decoder*. In each step, the *encoder* is trained first, and its weights are then fixed to generate the latent vector, which is passed to the *decoder*. The *decoder* is then updated, after which its weights are fixed for the next step of *encoder* training. This approach ensures that the *encoder* produces latent vectors that retain the structural information aligned with the GNN, allowing the *decoder* to reconstruct similar graph embeddings and yield comparable classification probabilities.

4.2.2 Fidelity Evaluation

To assess how removing each graphlet impacts the original classification probability, we introduce perturbations in the graphlet frequency vector as input to the surrogate model. We perform two inference runs for each graph. In the first, we use the original graphlet frequency vector to obtain the baseline classification confidence. This is essential because the surrogate model only approximates the GNN’s behavior, and this run establishes the comparison standard. In the second run, we use the perturbed graphlet frequency vector, simulating the removal of a graphlet and capturing the new classification confidence. The difference between the two confidence scores represents the fidelity metric, indicating the significance of the removed graphlet. The larger the score, the more crucial that graphlet is to the classification, as its removal significantly affects the result.

The perturbation applied to the graphlet frequency vectors involves setting the frequency of the targeted graphlet to zero. To account for the interdependencies between graphlets of different sizes, such as 4-node and 5-node graphlets, our method incorporates the hierarchical relationships among these substructures. For example, a 4-node star

graphlet is a subgraph of a 5-node star graphlet, so adjusting the frequency of the smaller graphlet requires updating the frequency of the larger one. When the 4-node star graphlet’s frequency is set to zero, the frequency of any containing graphlet, such as the 5-node star, must also be reduced to zero.

When targeting a 5-node star graphlet for perturbation (i.e., setting its frequency to zero), adjustments must also be made to the frequencies of 4-node star graphlet, as well as any other dependent 4-node graphlets that contribute to the formation of the 5-node star. This is essential because a 5-node star can be created by adding edges or nodes to any one of the dependent 4-node graphlets. To compute these adjustments, we apply a softmax function to the frequencies of all the related 4-node graphlets. This yields an estimate how much each 4-node graphlet contributes to forming the 5-node star. For each dependent 4-node graphlet, we subtract the frequency of the 5-node star, weighted by its softmaxed contribution. This adjustment process cascades down to interdependent graphlets, recalibrating the frequencies from 5-node to 4-node, and recursively from 4-node to 3-node graphlets. This ensures a consistent perturbation across interdependent substructures.

After applying perturbations (i.e., removing the target graphlet) to the graphlet frequency vector, we evaluate the impact by comparing the classification confidence before and after the removal. This is done by calculating the sum of the absolute values of the L1 distance between the two inference runs for each graph. A large L1 distance indicates that the removed graphlet is a key substructure, significantly affecting the GNN’s classification. To ensure accurate comparison, we use the confidence scores from the complete encoder-decoder model to project the graphlet frequency vector into the same graph embedding space as the GNN. This step helps to further minimize the slight discrepancies between the surrogate model and the GNN when calculating the L1 distance between their confidence scores.

To further validate the alignment between the surrogate model’s performance on the perturbed graphlet frequency vectors and the GNN’s behavior on the perturbed graphs, we identify the exact node and edge removals in each graph that would produce a graphlet frequency vector matching the one generated by our perturbation algorithm. Using the MUTAG dataset [6] as an example, we target the removal of a ring-structured graphlet. The graphlet frequency vectors resulting from direct node and edge removals in the original graphs show an average cosine similarity of 0.9996 to the graphlet frequency vectors generated by our perturbation algorithm. Additionally, the classification probabilities produced by the trained GNN on these directly perturbed graphs exhibit an average cosine similarity of 0.9449 with the classification probabilities from the trained surrogate model on the algorithm-perturbed graphlet frequency vectors. This experiment confirms that the surrogate model is well-trained to approximate GNN behavior and that its performance on the perturbed graphlet frequency vectors effectively mimics how the GNN would behave on the perturbed graphs.

4.3 Visual Analytics of GNNAnatomy

Our visual analytics system is a pivotal tool for interactively developing and evaluating explanations. It consists of four columns that facilitate the GNNAnatomy workflow, as shown in Fig. 5. Below, we provide a brief summary of the interface’s key functions and how they contribute to the overall workflow.

1. Beginning with the *Graph Group Selection* column (Fig. 5(a)), the *projection map* (Fig. 5(a2)) helps users identify graph groups that exhibit distinct topological features, which are critical for differentiating classes within each group. The selection made in Fig. 5(a2) can be further refined in Fig. 5(a3) based on the class and classification confidence of the selected graphs.
2. After selecting a group of graphs in Fig. 5(a), the *Substructure Explanatory Ranking* column (Fig. 5(b)) depicts each graphlet (Fig. 5(b1)), ranked based on its correlation with the GNN’s classifications. It also shows the class-wise distribution of graphs based on the frequency of each graphlet (Fig. 5(b2)).

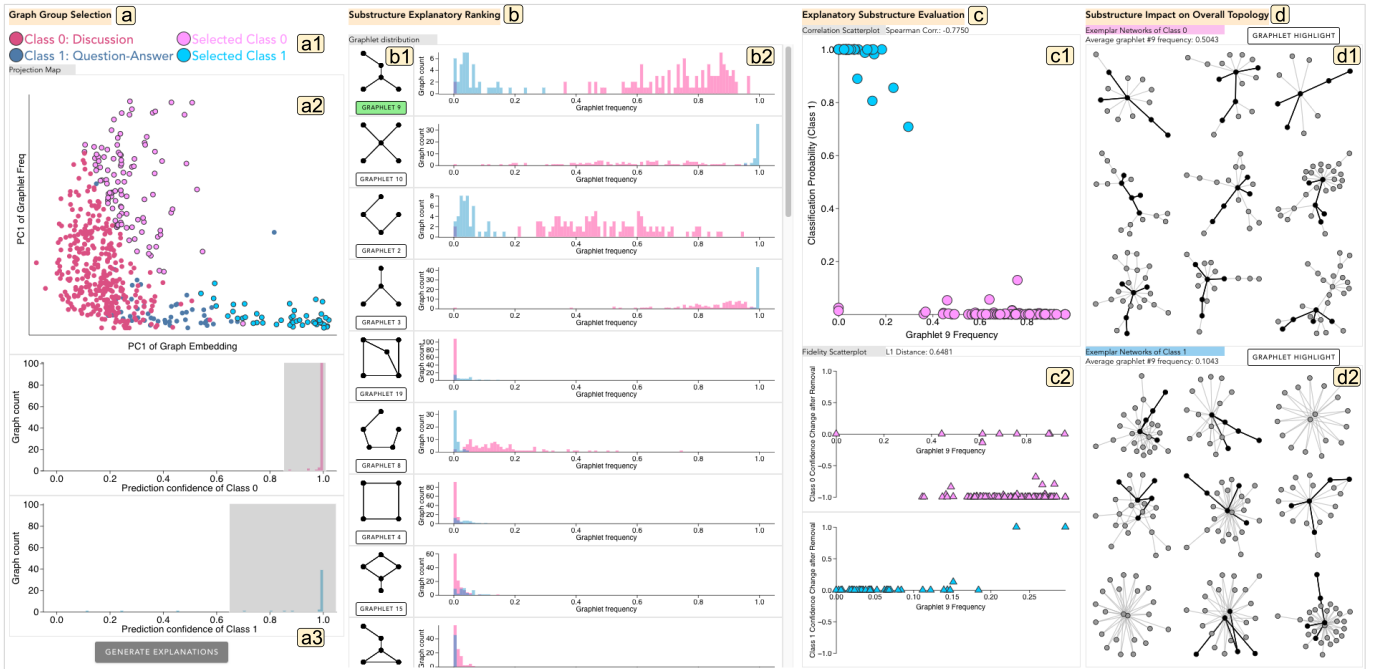


Fig. 5: The interface of GNNAnatomy, a screen capture of generating and reviewing explanations for the GNN behavior on a selected group of graphs from the Reddit-Binary dataset. In Column a, (a1) displays the legends for color encoding; (a2) shows the projection map visualizing the proximity of graphs, guiding users to select a group of graphs for which explanations are generated; and (a3) allows users to refine their selection based on class. After clicking the “generate explanation” button, Column b displays graphlets ranked according to their relevance to the GNN’s classifications; (b1) depicts each graphlet, while (b2) presents a class-specific histogram showing the distribution of graphs based on graphlet frequency. Subsequently, users can validate the relevance of a specific graphlet by selecting it, as shown in column (c), where *graphlet₉* is chosen; (c1) displays the correlation pattern between *graphlet₉*’s frequency and the classification probability, while (c2) illustrates the changes in classification confidence for each graph after removing *graphlet₉*. Users may lasso-select graphs in (c1) to see the overall topological impact of the chosen substructure, *graphlet₉*. In Column d, (d1) and (d2) then display representative graphs from two different classes, highlighting the topological differences due to the varying frequency of *graphlet₉*. Users can examine the occurrences of *graphlet₉* within each graph by clicking the “graphlet highlight” button.

- Upon selecting a graphlet in Fig. 5(b), the *Explanatory Substructure Evaluation* column (Fig. 5(c)) reveals the correlation between the frequency of the chosen graphlet and the GNN’s classification probability (Fig. 5(c1)). Fig. 5(c2) provides class-wise scatterplots illustrating changes in classification confidence when the selected graphlet is removed. Based on these patterns, users can then choose specific graphs to further examine their topology in Fig. 5(d).
- The *Substructure Impact on Overall Topology* column (Fig. 5(d)) illustrates how the selected graphlet affects the overall graph topology. A set of representative graphs from the two classes chosen in Fig. 5(c) is displayed (Fig. 5(d1, d2)). When the “graphlet highlight” button is clicked, the selected graphlet is highlighted in each graph where it appears. Clicking again highlights the next graphlet.

In this interface, the probability output for the class to which a graph belongs is referred to as *classification confidence*, while the probability output specifically for *Class₁* is termed *classification probability*. For instance, if a Discussion graph (i.e., *Class₀*) has a GNN probability output of $[0.75, 0.25]$, its classification confidence is 0.75 and its classification probability is 0.25. In the following paragraphs, we use this terminology to introduce each visual component in detail, highlighting the information each conveys.

4.3.1 Graph Group Selection

As shown in Fig. 5(a), this column consists of three components. First, Fig. 5(a1) displays the color legends used throughout the interface. Next, Fig. 5(a2) features the *Projection Map*, which projects all graphs from the analyzed dataset. The x-axis represents the first principal component (PC1) of the 80D graph embedding generated by the trained GNN. The proximity along the x-axis indicates how similarly the GNN perceives the graphs; graphs closer together are considered more similar in terms of the topological traits captured to generate their embeddings. The y-axis represents the PC1 of the 29D graphlet frequency vectors,

with proximity along this axis reflecting the similarity in graph topologies as characterized by the graphlets. Graphs closer on the y-axis have more similar topologies.

The relationship between these two sets of projections helps users identify graph groups that require distinct topological traits for class differentiation. For example, as shown in Fig. 5(a2), the diagonal selection indicates that graphs from two classes within this group exhibit notable structural differences, as evidenced by their separation along the y-axis. Additionally, the GNN is also able to distinguish between the two classes based on their separation along the x-axis. Thus, this selection allows users to investigate the salient structural difference that the GNN utilizes for class differentiation within this group. Conversely, Fig. 6(a) shows a group where the graphs from two classes have very similar topologies, as their graphlet frequency projections largely overlap. Despite this, the GNN can still differentiate between the classes because their PC1s of graph embeddings are separable along the x-axis. Hence, this selection enables users to explore the subtle structural differences between the classes captured by the GNN.

Guided by the associations revealed in the projection map, users can lasso-select a group of graphs for which explanations are generated, highlighted with pink and cyan outlines. Fig. 5(a3) allows for further refinement of this selection. The chosen graphs are displayed in two histograms, sorted by class label, showing their distribution across GNN-generated confidence scores. This refinement feature enables users to brush and select specific sections of confidence scores by class.

In summary, this column, specifically the projection map, enables the following generation of GNN explanations at various levels. Depending on the number of graphs selected, GNNAnatomy can provide explanations at the instance-, group-, or model- level.

4.3.2 Substructure Explanatory Ranking

As shown in Fig. 5(b), each graphlet is depicted in Fig. 5(b1) with a histogram in Fig. 5(b2) presenting the class-wise distribution of graphs

by frequency. The graphlet images provide an intuitive understanding of the substructures, while the histogram reveals differences in frequency domains across classes, helping users compare graphlet substructures and select one for further validation of its relevance to GNN behavior.

The ranking of graphlets (i.e., the order from top to bottom) is based on the absolute value of the Spearman’s correlation coefficient between each graphlet’s frequency and the GNN classification probabilities. We use Spearman’s correlation instead of another popular choice, Pearson’s, because the relationship between graphlet frequency and GNN classification probabilities is not necessarily linear. With 29 graphlets, the GNN may leverage their combined distinguishability to differentiate classes, making Spearman’s correlation a better fit for capturing non-linear associations.

4.3.3 Explanatory Substructure Evaluation

As shown in Fig. 5(c), we provide two visualizations: the correlation scatterplot in Fig. 5(c1) and the fidelity scatterplot in Fig. 5(c2).

Correlation scatterplot. In Fig. 5(c1), each graph in the selected group is plotted with the frequency of the chosen graphlet on the x-axis and the classification probability on the y-axis. This scatterplot helps users examine the correlation patterns, showing how well the chosen graphlet aligns with GNN behavior for class differentiation. The Spearman’s correlation coefficient, displayed above the scatterplot, provides a quantitative measure of this relationship.

Fidelity scatterplot. In Fig. 5(c2), each triangle represents a graph. The two scatterplots show the changes in classification confidence after removing the chosen graphlet from graphs of each class. These changes are based on confidence scores from two inferences of the trained surrogate model using original and perturbed graphs, as described in Sec. 4.2.2. The scatterplots differentiate between positive effects (improved confidence) and negative effects (decreased confidence) along the y-axis. The x-axis represents the frequencies of the selected graphlet in the original graphs. Additionally, the average change, calculated as the mean absolute L1 distance between original and perturbed classification confidences, is displayed above scatterplots, summarizing the impact of graphlet removal.

By employing graphlets as a diverse set of explanatory elements, our evaluation extends beyond comparing different explanation methods. Instead, our system adds a validation layer to the explaining process, allowing users to explore and interactively assess the relevance of all graphlets through metrics and visualizations. This collaborative approach to determining the explanation for the GNN inherently enhances its trustworthiness.

4.3.4 Substructure Impact on Overall Topology

Guided by the correlation patterns in Fig. 5(c1), users select graphs to analyze how variations in the frequency of the chosen graphlet affect the overall graph topology. In Fig. 5(d), two sets of network visualizations are provided: one for representative graphs of $Class_0$ and the other for $Class_1$. For each class, if more than nine graphs are selected, nine are randomly picked among the selected. Displaying an ensemble of nine graphs per class allows users to explore a variety of graph structures within the selected range while preserving visual clarity. These visualizations illustrate the impact of the chosen graphlet’s frequency on graph topology. The average frequency of the chosen graphlet is displayed above the visualizations to aid in comparison. This approach helps users understand how the substructural impact translates to overall topology differences and reason about the semantics of the explanatory graphlet, aided by the graph labels.

Clicking the “graphlet highlight” button will highlight one instance of the selected graphlet substructure in opaque black. Since each graph’s topology may contain multiple substructures, clicking the button again will highlight the next matching substructure, if available. This feature helps users locate graphlets in more complex topologies.

5 CASE STUDIES

We demonstrate the capabilities of GNNAnatomy through case studies using both real-world and synthetic graph datasets. Additionally, the generated explanatory substructures are quantitatively evaluated and

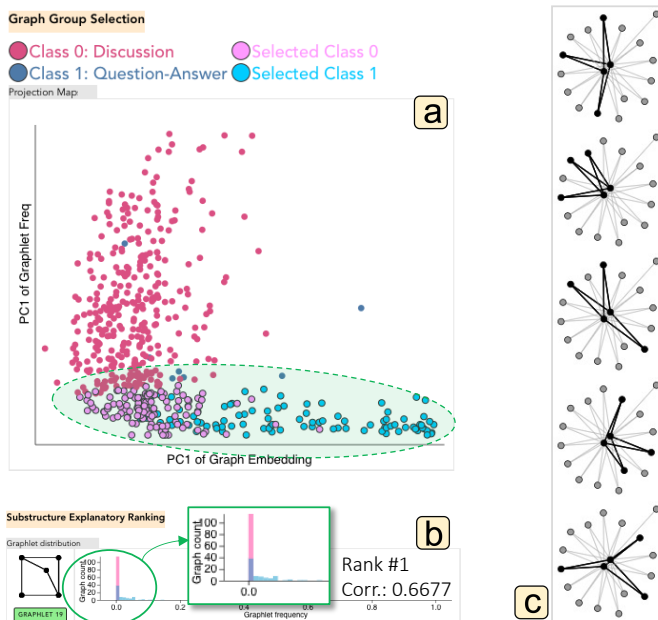


Fig. 6: (a) illustrates the selection of a group of graphs with similar topologies, aimed at observing subtle topological differences between the two classes in the Reddit-Binary dataset. (b) depicts the top-ranked $graphlet_{19}$ and the graph distribution over its frequency. (c) shows five examples where $graphlet_{19}$ locates in a representative Question-Answer graph.

qualitatively compared to those generated by other explainable GNN methods.

5.1 Experimental Settings

5.1.1 Datasets

Real-world datasets. We apply GNNAnatomy to explain GNN’s behavior on two real-world graph classification datasets. **Reddit-Binary** [45] comprises 2000 graphs, each representing a discussion thread extracted from Reddit. In these graphs, nodes correspond to users engaging in the thread, while edges denote replies between users’ comments. The graphs are labeled based on the nature of user interactions observed in the threads. Specifically, the dataset distinguishes between two types of interactions: Question-Answer, extracted from the subreddits $r/IAmA$ and $r/AskReddit$, and Discussion, logged from the subreddits $r/Tro1LXChromosomes$ and $r/atheism$. **MUTAG** [6] consists of 188 molecule graphs, each labeled based on its mutagenic effect on the Gram-negative bacterium *Salmonella typhimurium*.

Synthetic dataset. We also evaluate the performance of GNNAnatomy using a synthetic graph classification dataset introduced in [27], **BA-2Motif**. BA-2Motif contains 1000 graphs, where each constitutes a base graph generated by the Barabasi-Albert (BA) random graph model. Half BA base graphs are attached with a house motif and the other half is attached with a 5-node cycle motif, as illustrated in Fig. 11. Each graph in BA-2Motif comprises of 25 nodes and is assigned to one of the two classes based on the motif attached.

5.1.2 Graph Neural Network (GNN)

We use the Graph Convolutional Network (GCN) [18] as the GNN model to be explained on the selected datasets. GCN is chosen because shares the same learned weights for aggregating information from same-hop neighbors across the entire graph. This ensures that identical substructures are valued consistently, no matter where they appear within a graph. To emphasize the aggregation of structural information, we omit any node or edge attributes and instead utilize the one-hot encoding of node degrees as the initial vector for each node. Our GCN architecture consists of four convolutional layers that aggregate information from neighboring nodes, followed by a fully connected layer for classification. The output from each convolutional layer, with

a dimensionality of 20, is concatenated to create an 80-dimensional node embedding for each graph. All node embeddings within a graph are then aggregated to form an 80-dimensional graph embedding.

The decision to use a 4-layer architecture is directly linked to our use of graphlets. Since the largest diameter among the graphlets is 4 (specifically, the 5-node acyclic graphlet), the GNN must aggregate information from neighbors up to 4 hops away to capture the topological characteristics of these 5-node substructures. Additionally, by concatenating the outputs of each convolutional layer to form the graph embeddings, we allow the graph embeddings to reflect substructures captured from lower-hop neighbors. This approach helps reduce any bias toward the 5-node structures, which might otherwise dominate in the final layer of the GNN, ensuring a more balanced representation of the various substructures within the graph.

5.1.3 Baselines

We choose to compare the explanations generated by our GNNAnatomy with those provided by MotifExplainer [49], which aims to identify general motifs as explanations. Additionally, we include GNNExplainer [47], since it has been widely used as a common baseline in nearly every other explainable GNN studies [14, 27, 27, 43, 49, 52] and its authors inferred class motifs from the instance-level explanation subgraphs generated by this method. The comparison is made based on the availability of explanations in the original baseline papers as indicated in Table 1.

| | Reddit-Binary | MUTAG | BA-2Motif |
|----------------|---------------|-------|-----------|
| Ground Truth | - | ✓ | ✓ |
| GNNExplainer | ✓ | ✓ | - |
| MotifExplainer | - | ✓ | ✓ |

Table 1: The availability of explanations in each original baseline paper.

5.1.4 Evaluation Metrics

GNNAnatomy generates substructure explanations that highlight the importance of topological traits rather than the significance of individual nodes and edges. As a result, common metrics are generally not applicable to GNNAnatomy, and vice versa. For instance, the ROC-AUC metric [47] requires ground truth and subgraph-formatted explanations to measure the exact alignment of nodes and edges. Similarly, the Fidelity [31] metric requires removing nodes and edges deemed highly important by the explainable GNN method. Therefore, we evaluate the validity of our substructure explanations by utilizing the Spearman’s correlation and adapting the concept of the Fidelity metric to quantify the impact of removing each graphlet on the GNN’s classification, as introduced in Sec. 4.2.2.

5.2 Study 1: Reddit-Binary

GNN training results. Due to the computational cost associated with graphlet frequency calculation, we only use 554 graphs with fewer than 100 nodes for training, inference, and explaining. Among the 554 graphs, consisting of 101 graphs of the Question-Answer (QA) class and 453 graphs of the Discussion class, the GNN model achieves a classification accuracy of 0.9549 (i.e., over 0.5 confidence score), and the classification probabilities output by the surrogate model exhibit a cosine similarity of 0.9322 with the GNN probabilities output.

GNNAnatomy explanations. As depicted in Fig. 5(a2), a group of graphs with distinct topologies and graph embeddings (i.e., separated PCs of both graphlet frequency vectors and graph embeddings) is selected. This selection aims to identify the salient substructure differences between the two classes that are relevant to the GNN behavior. This selection is further refined in Fig. 5(a3) to include only those graphs classified with high confidence. In Fig. 5(b2), the distribution of the top-ranked graphlet, *graphlet*₉, shows clear separation across classes. This suggests that classifying graphs based solely on the frequency of *graphlet*₉ could potentially achieve the same high classification accuracy as the GNN, which marks its distinguishability.

In Fig. 5(c1), a strong negative correlation (Spearman correlation corr.: -0.74) between the frequency of *graphlet*₉ and the classification probability is shown. Furthermore, in Fig. 5(c2), the necessity of

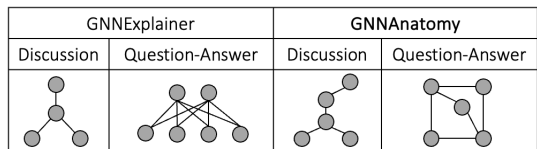


Fig. 7: Reddit-Binary dataset. The class motifs inferred by GNNExplainer and substructure explanations generated GNNAnatomy.

*graphlet*₉ in maintaining the current GNN classifications is confirmed. Upon removal of *graphlet*₉, the confidence scores of Discussion graphs decrease while those of QA graphs with unusually high frequencies of *graphlet*₉ increase. These changes indicate that the GNN tends to classify most graphs as QA graphs when *graphlet*₉ is absent from their topologies, thereby validating the relevance of *graphlet*₉ to GNN behavior. The visualizations of representative graphs from the two classes show that *graphlet*₉ is a more communicated substructure in Discussion graphs, where they have larger number of occurrence as shown in Fig. 5(d1). While in QA graphs as illustrated in Fig. 5(d2), some of them are completely free of the *graphlet*₉ substructure (i.e., the two graphs without any highlights on their topology). Connecting to the semantics of the Discussion label, a deeper insight reveals that *graphlet*₉ captures unique branched-out characteristic in common discussions.

As shown in Fig. 6(a), another selected group of graphs is investigated to uncover subtle topological disparities between classes that aid in the GNN’s classification effectiveness. As depicted in Fig. 6(b), the frequency of the top-ranked *graphlet*₁₉ correlates with the GNN classification probability with a correlation coefficient of 0.6677. Additionally, the representative network visualization also shows abundant *graphlet*₁₉ occurrences, as highlighted in Fig. 6(c). The two distinct explanations for the two respective groups suggest a reasoning process for the GNN: while the structural trait of Discussion graphs (i.e., *graphlet*₉) is sufficient to distinguish most graphs, when classifying graphs with very similar topologies, the structural trait of QA graphs becomes the next indicator that the GNN relies on.

In summary, it is evident that GNN employs different substructures to classify different groups of graphs. GNNAnatomy not only helps users identify these groups but also correctly attributes the relevance of graphlets using correlation and fidelity metric.

Qualitative evaluation. The Reddit-Binary dataset lacks ground truth motifs for each class, but GNNExplainer [47] derives a motif for each class, which has been used as a comparison baseline. As shown in Fig. 7, our graphlet explanation for the Discussion class includes an additional edge and node compared to the motif proposed by GNNExplainer. For the QA class, our graphlet explanation aligns with GNNExplainer’s motif, as both depict a substructure where two sets of nodes are fully connected to another set.

The additional node and edge in our Discussion explanation uniquely capture the presence of the branching characteristic more commonly found in discussion graphs. In contrast, the Discussion motif proposed by GNNExplainer appears not only in typical Discussion graphs but also significantly in QA graphs. As shown in Fig. 6(c), the 4-node star pattern—where one of two central nodes connects to three peripheral nodes—is prevalent, even in a representative QA graph. This highlights the indistinguishability of GNNExplainer’s Discussion motif. Moreover, our explanations are mutually exclusive, as a 5-node connected substructure is classified as only one type of 5-node graphlet. This underscores the distinct class-wise patterns captured by GNNAnatomy. It is also crucial to recognize that merely presenting the common topological patterns of each class does not fully explain GNN behavior. As demonstrated in this study, different explanations apply to different groups of graphs.

5.3 Study 2: MUTAG

GNN training results. By relying solely on topological characteristics, the GNN learns to classify a molecule’s mutagenicity (i.e., a binary classification of mutagen or non-mutagen). The trained GNN achieves a classification accuracy of 0.8191, while the surrogate model shows a cosine similarity of 0.9939 with the GNN’s probability output. To

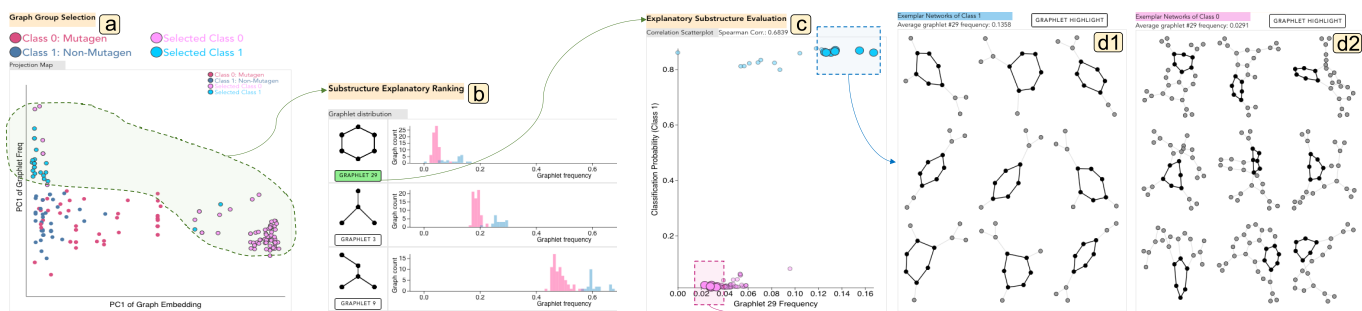


Fig. 8: Starting from (a), a group of graphs is selected to investigate the key structural differences between mutagens and non-mutagens. In (b), each graphlet is ranked according to its relevance to the GNN’s classifications. After selecting the top-ranked ring graphlet, (c) shows a scatterplot illustrating the correlation between the frequency of the ring graphlet and the classification probability. With the graphs having contrasting graphlet frequencies chosen, (d1) and (d2) reveal the overall topology reflecting this frequency difference and highlight the ring graphlet within their topology.

demonstrate the flexibility of GNNAnatomy, a 6-node ring-structured graphlet is also incorporated to characterize graph topology, as it has been identified by domain experts as a key structure in mutagenic compounds [6].

GNNAnatomy explanations. From Fig. 8(a), a group of graphs with distinct topologies and graph embeddings is chosen. This selection, similar to Study 1, enables the investigation of salient topological differences that help the GNN distinguish between the two classes. Ranked as the most relevant in Fig. 8(b), the 6-node ring-structured graphlet (i.e., *graphlet*₂₉) serves as the explanatory substructure for this group, with its frequency distribution distinguishing between the two classes. As introduced in Sec. 4.1, this distinguishability may arise from differences in the number of nodes in the graphs, the number of 6-node connected subgraphs sampled from each graph, or the number of occurrence of *graphlet*₂₉ in each graph. To identify which factor contributes to this distinguishability, we synthesize a dataset, *syn_rings*, containing graphs constructed from varying numbers of 6-node rings (i.e., *graphlet*₂₉), ranging from 1 to 7 and combined only in patterns found in the original MUTAG dataset. In *syn_rings*, an increase in the number of rings within a graph results in a lower frequency of *graphlet*₂₉ due to the corresponding rise in the total number of nodes. Additionally, in the MUTAG dataset, the two classes show a statistically significant difference in their distributions of ring occurrences. The Kolmogorov–Smirnov (KS) test yields a score of 0.52 with a p-value of 7.7×10^{-11} . This confirms a connection between the number of ring occurrences and the frequency of *graphlet*₂₉. Specifically, mutagen graphs tend to exhibit more rings in their topology and a lower frequency of *graphlet*₂₉ compared to non-mutagen graphs. Additionally, the frequency of *graphlet*₂₉ shows a strong correlation with the GNN’s classification probability, with a Spearman’s correlation coefficient of 0.6839, as demonstrated in Fig. 8(c).

In Fig. 8(c), we selected graphs with contrasting frequencies of *graphlet*₂₉ to examine the typical structural characteristics of each class. In Fig. 8(d1), it is evident that typical non-mutagen graphs tend to have only one ring (i.e., *graphlet*₂₉), while mutagen graphs, as shown in Fig. 8(d2), feature more rings fused together in their topology. Thus, the key difference between the two classes appears to be the number of fused rings, rather than just the presence of a ring. To validate this observation, we examine the graphs in *syn_rings*, where the rings are fused in patterns consistent with those found in the original MUTAG dataset. In *syn_rings*, an increase in the number of fused rings results in a lower frequency of *graphlet*₂₉, which aligns the lower frequency distribution seen in mutagen graphs. This further assures that the distinguishing topological trait between mutagen and non-mutagens is the number of fused rings.

Qualitative evaluation. As indicated in Table 1, we compare our explanations to the ground truth and those generated by GNNExplainer [47] and MotifExplainer [49]. According to domain experts [6], the compounds likely to induce a mutagenic effect on the Gram-negative bacterium *S. typhimurium* include 6-node carbon rings, fused carbon rings, and NO_2 . In GNNAnatomy, the 6-node ring graphlet emerges as the most relevant substructure, while the second and third

| Ground Truth | GNNExplainer | MotifExplainer | GNNAnatomy |
|--------------|--------------|----------------|------------|
| | | | |

Fig. 9: MUTAG dataset. The ground truth mutagenic compounds, which include a fused ring, a 6-node ring structure, and NO_2 (from right to left), along with the explanations provided by the baseline methods and GNNAnatomy.

most relevant graphlets, as shown in Fig. 8(b), correspond to NO_2 structures. Furthermore, our visual analytics system highlights the mutagenicity associated with an increased number of rings fused together. Thus, GNNAnatomy successfully captures the importance of all three ground truth substructures. In contrast, as summarized in Fig. 9, GNNExplainer [47] identifies the importance of both 6-node ring subgraphs and NO_2 compounds but fails to detect the key distinguishing factor of fused rings between the two classes. Similarly, MotifExplainer [49] identifies only the NO_2 compound, overlooking the significance of the 6-node rings. To our knowledge, GNNAnatomy is the only explainer capable of capturing the importance of structural traits that require more rings fused together for a mutagen to become distinguishable.

5.4 Study 3: BA-2Motif

GNN training results. The GNN is trained to classify which motif (i.e., a 5-node house or a 5-node cycle) is attached to a BA base graph. The GNN model achieves a classification accuracy of 1.0, while the surrogate model shows a cosine similarity of 0.9681 with the GNN probability output.

GNNAnatomy explanations. In Fig. 10(a1), we observe that the PC1s of the graphlet frequency vectors for graphs from different classes span a similar domain, as the two classes differ by only a single edge in their attached motifs. Therefore, we select the entire dataset to examine the subtle topological differences captured by the GNN. In Fig. 10(a2), the top three relevant graphlets highlight a strong emphasis on the triangle substructure. Upon selecting the triangle graphlet (i.e., *graphlet*₁), its significance is confirmed by a strong correlation of 0.7887 between its frequency and the GNN’s classification probability, as shown in Fig. 10(a3). Moreover, the classification confidence for the House class graphs drops by 0.3052 when the triangle substructure is removed from their topology, as depicted in Fig. 10(a4). These findings demonstrate the distinguishability of the triangle structure between the House and Cycle classes.

As shown in Fig. 10(b), we verify that triangles are typically absent in any BA base graphs, making a triangle a unique substructure that appears only in house motifs, and therefore, a distinctive topological trait of House class graphs. This observation aligns with the fact that all Cycle class graphs have zero frequency (i.e., zero occurrences) of any triangle-containing graphlets, as indicated in Fig. 10(a2). However, since a house motif consists of a triangle merged with a rectangle, it is natural to question why the rectangle is not the most relevant substructure. In Fig. 10(b), it is clear that the node connecting to the base graph is contained within the triangle. From this connecting

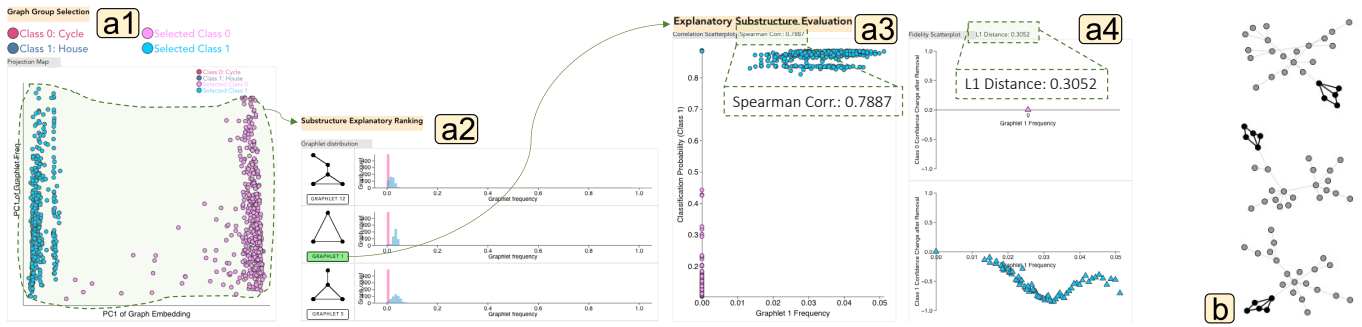


Fig. 10: In (a1), a group of graphs is selected to examine the subtle structural differences between House class graphs and Cycle class graphs. (a2) highlights the strong relevance of the triangle substructure. Upon selecting the triangle graphlet, (a3) displays a scatterplot showing the strong correlation between the frequency of the triangle graphlet and the classification probability of House graphs. Additionally, (a4) shows a decrease in the classification probability of House graphs after the triangle graphlet is removed. (b) illustrates how house motifs are attached to BA base graphs, with the house motifs highlighted.

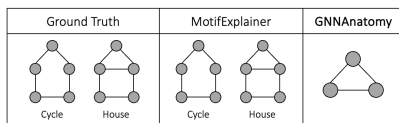


Fig. 11: BA-2Motif dataset. The ground truth motifs and the explanations generated by a baseline and GNNAnatomy.

node, a triangle substructure requires only one hop to be completed, whereas a rectangle requires one and two hop neighbors to be completed. The stronger relevance of triangle-containing graphlets to the GNN’s classifications suggests that the GNN learns to utilize only the minimum amount of information needed for class differentiation (i.e., the triangle substructure rather than the rectangle substructure).

Qualitative evaluation. In Fig. 11, the explanations generated by MotifExplainer [49] align with the ground truth motifs attached to the BA base graphs. However, MotifExplainer does not assess the relevance of the elementary substructures within their defined motifs. Therefore, the measured importance needs to be further broken down into each elementary substructure, such as a triangle or rectangle within a house motif. In contrast, GNNAnatomy incorporates diverse graphlets with varying numbers of nodes, allowing it to characterize graph topology at multiple levels of granularity. As a result, our method more accurately reveals GNN behavior by capturing the stronger relevance of triangle-containing graphlets over the complete house motif.

6 DISCUSSION AND FUTURE WORKS

6.1 Scalability in Graphlet Frequency Computation

Using 3-, 4-, and 5-node graphlets ensures a diverse range of substructures while keeping the total number of graphlets computationally manageable and perceivable by users. For example, in a graph with 94 nodes and 222 edges, efficient sampling method proposed in [36] yields 1106, 15113, and 172127 sampled 3-, 4-, and 5-node connected subgraphs, respectively. To compute each graphlet’s frequency in a graph, we iterate over these samples, checking for isomorphism with the target graphlet. Although random sampling was attempted, it compromised frequency precision. While this process can be time-consuming for larger networks, it is a one-time operation per dataset and could be expedited by segmenting graphs into smaller components before sampling. To make GNNAnatomy more efficient for other datasets, we are developing a benchmark with graphlet frequency vectors for popular graph datasets.¹

6.2 Generalizability

Other GNN models. GNNAnatomy functions as a post-hoc method, utilizing graph embeddings and softmax probabilities produced by a trained graph convolutional network (GCN). As a result, it can be applied to any GNN that generates graph embeddings for individual graphs.

¹The graphlet frequency of graphs in the three datasets used in our case studies will be made available upon publications.

Multi-class graph classification tasks. Although we showcase GNNAnatomy’s capabilities with binary classification datasets, our approach can be extended to multi-class classification tasks. A key algorithmic adjustment would involve computing correlations between two classes at a time, then using a statistical summary of pairwise correlation coefficients to rank the relevance of graphlets.

Node classification tasks. While GNNAnatomy is primarily designed for graph classification tasks, its methodology could potentially be adapted to explain GNN behavior in node classification tasks. Instead of using graph embeddings and classification probabilities, node embeddings and node classification probabilities could be employed. For graphlet frequency, we could track how often a specific node appears in a certain graphlet type, such as *graphlet*₂₀, relative to all occurrences of *graphlet*₂₀ in the original graph. This approach would help identify a node’s role within the overall graph topology through the lens of graphlet representation.

Domain-specific Motifs. As discussed in Sec. 5.3, if a domain-specific substructure, such as a 6-node ring, is hypothesized to explain the GNN’s behavior but is not included in the default set of graphlets, users can easily add it to the analysis. Additionally, since graphlets are interdependent, even if the hypothesized graphlet is not explicitly included, there would still be evidence suggesting a potential explanation. Users can then incorporate that graphlet into the analysis to verify the hypothesis. Furthermore, as demonstrated in Sec. 5.4, the interdependency of graphlets allows users to break down the relevance of a domain-specific motif (such as the house motif) into its sub-components (such as the triangle and rectangle within the house motif).

6.3 Extensibility

As discussed in Sec. 5.2, GNN utilizes *graphlet*₉ and *graphlet*₁₉ to classify different groups of graphs. In other graph datasets, different dominant graphlets may facilitate class differentiation for each selected group. This insight points to a potential extension of our work: developing a decision tree that hierarchically outlines the substructure criteria GNNs use at each step to reach their final classification. We intend to explore this application in future research.

7 CONCLUSION

We introduce a novel explainable GNN method designed to systematically generate and evaluate substructure explanations that align with GNN behavior at desired levels. Our approach utilizes graphlets to create substructure explanations and employs correlation and fidelity metric to assess their validity. We integrate interactive visualizations to streamline the process of crafting trustworthy explanations. Through case studies on real-world and synthetic graph datasets from various domains, we demonstrate the efficacy of GNNAnatomy and compare the quality of our explanations to state-of-the-art explainable GNN approaches. While showcasing the versatility and utility of our method, we outline future research directions for extending GNNAnatomy.

REFERENCES

- [1] A. M. Abbas. Social network analysis using deep learning: applications and schemes. *Social Network Analysis and Mining*, 11(1):106, 2021. 1
- [2] M. Bajaj, L. Chu, Z. Y. Xue, J. Pei, L. Wang, P. C.-H. Lam, and Y. Zhang. Robust counterfactual explanations on graph neural networks. *Advances in Neural Information Processing Systems*, 34:5644–5655, 2021. 1, 2
- [3] G. Bouritsas, F. Frasca, S. Zafeiriou, and M. M. Bronstein. Improving graph neural network expressivity via subgraph isomorphism counting. *IEEE Transactions on Pattern Analysis and Machine Intelligence*, 45(1):657–668, 2022. 2, 3
- [4] J. Chen, S. Wu, A. Gupta, and R. Ying. D4explainer: In-distribution explanations of graph neural network via discrete denoising diffusion. *Advances in Neural Information Processing Systems*, 36, 2024. 1, 2
- [5] T. Chen, S. Kornblith, M. Norouzi, and G. Hinton. A simple framework for contrastive learning of visual representations. In *International conference on machine learning*, pp. 1597–1607. PMLR, 2020. 2, 3
- [6] A. K. Debnath, R. L. Lopez de Compadre, G. Debnath, A. J. Shusterman, and C. Hansch. Structure-activity relationship of mutagenic aromatic and heteroaromatic nitro compounds. correlation with molecular orbital energies and hydrophobicity. *Journal of medicinal chemistry*, 34(2):786–797, 1991. 2, 4, 6, 8
- [7] J. Degen, C. Wegscheid-Gerlach, A. Zaliani, and M. Rarey. On the art of compiling and using ‘drug-like’ chemical fragment spaces. *ChemMedChem*, 3(10):1503, 2008. 2
- [8] X. T. Dinh and H. Van Pham. Social network analysis based on combining probabilistic models with graph deep learning. In *Communication and Intelligent Systems: Proceedings of ICCIS 2020*, pp. 975–986. Springer, 2021. 1
- [9] K. Faust. A puzzle concerning triads in social networks: Graph constraints and the triad census. *Social Networks*, 32(3):221–233, 2010. 3
- [10] R. C. Fong and A. Vedaldi. Interpretable explanations of black boxes by meaningful perturbation. In *Proceedings of the IEEE international conference on computer vision*, pp. 3429–3437, 2017. 3
- [11] T. Funke, M. Khosla, and A. Anand. Hard masking for explaining graph neural networks. 2020. 1, 2
- [12] F. Heimerl, C. Kralj, T. Möller, and M. Gleicher. embcomp: Visual interactive comparison of vector embeddings. *IEEE Transactions on Visualization and Computer Graphics*, 28(8):2953–2969, 2020. 3
- [13] S. Hooker, D. Erhan, P.-J. Kindermans, and B. Kim. A benchmark for interpretability methods in deep neural networks. *Advances in neural information processing systems*, 32, 2019. 1, 2
- [14] Q. Huang, M. Yamada, Y. Tian, D. Singh, and Y. Chang. Graphlime: Local interpretable model explanations for graph neural networks. *IEEE Transactions on Knowledge and Data Engineering*, 2022. 1, 2, 7
- [15] S. Jin, X. Zeng, F. Xia, W. Huang, and X. Liu. Application of deep learning methods in biological networks. *Briefings in bioinformatics*, 22(2):1902–1917, 2021. 1
- [16] W. Jin, R. Barzilay, and T. Jaakkola. Junction tree variational autoencoder for molecular graph generation. In *International conference on machine learning*, pp. 2323–2332. PMLR, 2018. 2, 3
- [17] Z. Jin, Y. Wang, Q. Wang, Y. Ming, T. Ma, and H. Qu. Gnnlens: A visual analytics approach for prediction error diagnosis of graph neural networks. *IEEE Transactions on Visualization and Computer Graphics*, 2022. 3
- [18] T. N. Kipf and M. Welling. Semi-supervised classification with graph convolutional networks. *arXiv preprint arXiv:1609.02907*, 2016. 1, 6
- [19] O. Kwon, T. Crnovrsanin, and K. Ma. What would a graph look like in this layout? A machine learning approach to large graph visualization. *IEEE Trans. Vis. Comput. Graph.*, 24(1):478–488, 2018. doi: 10.1109/TVCG.2017.2743858 3
- [20] B. La Rosa, G. Blasilli, R. Bourqui, D. Auber, G. Santucci, R. Capobianco, E. Bertini, R. Giot, and M. Angelini. State of the art of visual analytics for explainable deep learning. In *Computer Graphics Forum*, vol. 42, pp. 319–355. Wiley Online Library, 2023. 3
- [21] X. Q. Lewell, D. B. Judd, S. P. Watson, and M. M. Hann. Recap retrosynthetic combinatorial analysis procedure: a powerful new technique for identifying privileged molecular fragments with useful applications in combinatorial chemistry. *Journal of chemical information and computer sciences*, 38(3):511–522, 1998. 2
- [22] Q. Li, K. S. Njotoprawiro, H. Haleem, Q. Chen, C. Yi, and X. Ma. Embeddingvis: A visual analytics approach to comparative network embedding inspection. In *2018 IEEE Conference on Visual Analytics Science and Technology (VAST)*, pp. 48–59. IEEE, 2018. 3
- [23] R. Li, X. Yuan, M. Radfar, P. Marendy, W. Ni, T. J. O’Brien, and P. M. Casillas-Espinosa. Graph signal processing, graph neural network and graph learning on biological data: a systematic review. *IEEE Reviews in Biomedical Engineering*, 16:109–135, 2021. 1
- [24] Z. Liu, Y. Wang, J. Bernard, and T. Munzner. Visualizing graph neural networks with corgie: Corresponding a graph to its embedding. *IEEE Transactions on Visualization and Computer Graphics*, 28(6):2500–2516, 2022. 3
- [25] A. Lucic, M. A. Ter Hoeve, G. Tolomei, M. De Rijke, and F. Silvestri. CF-GNNexplainer: Counterfactual explanations for graph neural networks. In *International Conference on Artificial Intelligence and Statistics*, pp. 4499–4511. PMLR, 2022. 1, 2
- [26] S. Lundberg. A unified approach to interpreting model predictions. *arXiv preprint arXiv:1705.07874*, 2017. 3
- [27] D. Luo, W. Cheng, D. Xu, W. Yu, B. Zong, H. Chen, and X. Zhang. Parameterized explainer for graph neural network. *Advances in neural information processing systems*, 33:19620–19631, 2020. 1, 2, 3, 6, 7
- [28] S. Min, Z. Gao, J. Peng, L. Wang, K. Qin, and B. Fang. Stgsn—a spatial-temporal graph neural network framework for time-evolving social networks. *Knowledge-Based Systems*, 214:106746, 2021. 1
- [29] G. Muzio, L. O’Bray, and K. Borgwardt. Biological network analysis with deep learning. *Briefings in bioinformatics*, 22(2):1515–1530, 2021. 1
- [30] T. Pereira, E. Nascimento, L. E. Resck, D. Mesquita, and A. Souza. Distill n’explain: explaining graph neural networks using simple surrogates. In *International Conference on Artificial Intelligence and Statistics*, pp. 6199–6214. PMLR, 2023. 1, 2
- [31] P. E. Pope, S. Kolouri, M. Rostami, C. E. Martin, and H. Hoffmann. Explainability methods for graph convolutional neural networks. In *Proceedings of the IEEE/CVF conference on computer vision and pattern recognition*, pp. 10772–10781, 2019. 1, 2, 4, 7
- [32] N. Pržulj. Biological network comparison using graphlet degree distribution. *Bioinformatics*, 23(2):e177–e183, 2007. 3
- [33] M. T. Ribeiro, S. Singh, and C. Guestrin. " why should i trust you?" explaining the predictions of any classifier. In *Proceedings of the 22nd ACM SIGKDD international conference on knowledge discovery and data mining*, pp. 1135–1144, 2016. 3
- [34] B. Sanchez-Lengeling, J. Wei, B. Lee, E. Reif, P. Wang, W. Qian, K. McCloskey, L. Colwell, and A. Wiltschko. Evaluating attribution for graph neural networks. *Advances in neural information processing systems*, 33:5898–5910, 2020. 1, 2
- [35] M. S. Schlichtkrull, N. D. Cao, and I. Titov. Interpreting graph neural networks for {nlp} with differentiable edge masking. In *International Conference on Learning Representations*, 2021. 1, 2, 3
- [36] N. Shervashidze, S. Vishwanathan, T. Petri, K. Mehlhorn, and K. Borgwardt. Efficient graphlet kernels for large graph comparison. In *Artificial intelligence and statistics*, pp. 488–495. PMLR, 2009. 3, 9
- [37] Q. Tan, N. Liu, and X. Hu. Deep representation learning for social network analysis. *Frontiers in big Data*, 2:2, 2019. 1
- [38] J. Ugander, L. Backstrom, and J. Kleinberg. Subgraph frequencies: Mapping the empirical and extremal geography of large graph collections. In *Proceedings of the International Conference on World Wide Web*, p. 1307–1318, 2013. 3
- [39] M. Vu and M. T. Thai. Pgm-explainer: Probabilistic graphical model explanations for graph neural networks. *Advances in neural information processing systems*, 33:12225–12235, 2020. 1, 2
- [40] J. Wang, S. Liu, and W. Zhang. Visual analytics for machine learning: A data perspective survey. *IEEE Transactions on Visualization and Computer Graphics*, 2024. 3
- [41] Q. Wang, K. Huang, P. Chandak, M. Zitnik, and N. Gehlenborg. Extending the nested model for user-centric xai: A design study on gnn-based drug repurposing. *IEEE Transactions on Visualization and Computer Graphics*, 29(1):1266–1276, 2022. 3
- [42] X. Wang, Y. Wu, A. Zhang, X. He, and T.-s. Chua. Causal screening to interpret graph neural networks. 2020. 1, 2
- [43] X. Wang, Y. Wu, A. Zhang, X. He, and T.-S. Chua. Towards multi-grained explainability for graph neural networks. *Advances in Neural Information Processing Systems*, 34:18446–18458, 2021. 1, 2, 3, 7
- [44] H. Xuanyuan, P. Barbiero, D. Georgiev, L. C. Magister, and P. Liò. Global concept-based interpretability for graph neural networks via neuron analysis. In *Proceedings of the AAAI Conference on Artificial Intelligence*, vol. 37, pp. 10675–10683, 2023. 1, 2
- [45] P. Yanardag and S. Vishwanathan. Deep graph kernels. In *Proceedings of the 21th ACM SIGKDD international conference on knowledge discovery*

and data mining, pp. 1365–1374, 2015. 6

- [46] J. Yin, C. Li, H. Yan, J. Lian, and S. Wang. Train once and explain everywhere: Pre-training interpretable graph neural networks. *Advances in Neural Information Processing Systems*, 36:35277–35299, 2023. 1, 2, 4
- [47] Z. Ying, D. Bourgeois, J. You, M. Zitnik, and J. Leskovec. GNNExplainer: Generating explanations for graph neural networks. *Advances in neural information processing systems*, 32, 2019. 1, 2, 7, 8
- [48] Z. Ying, J. You, C. Morris, X. Ren, W. Hamilton, and J. Leskovec. Hierarchical graph representation learning with differentiable pooling. *Advances in neural information processing systems*, 31, 2018. 1
- [49] Z. Yu and H. Gao. Motifexplainer: a motif-based graph neural network explainer. *arXiv preprint arXiv:2202.00519*, 2022. 1, 2, 4, 7, 8, 9
- [50] H. Yuan, J. Tang, X. Hu, and S. Ji. Xgnn: Towards model-level explanations of graph neural networks. In *Proceedings of the 26th ACM SIGKDD International Conference on Knowledge Discovery & Data Mining*, pp. 430–438, 2020. 2
- [51] H. Yuan, H. Yu, S. Gui, and S. Ji. Explainability in graph neural networks: A taxonomic survey. *IEEE Transactions on Pattern Analysis and Machine Intelligence*, 2022. 2
- [52] H. Yuan, H. Yu, J. Wang, K. Li, and S. Ji. On explainability of graph neural networks via subgraph explorations. In *International conference on machine learning*, pp. 12241–12252. PMLR, 2021. 1, 2, 7
- [53] Y. Zhang, D. Defazio, and A. Ramesh. Relx: A model-agnostic relational model explainer. In *Proceedings of the 2021 AAAI/ACM Conference on AI, Ethics, and Society*, pp. 1042–1049, 2021. 1, 2